A Generative Model for Automatic Detection of Resolving Multiple Sclerosis Lesions

Colm Elliott[1], Douglas L. Arnold[3], D. Louis Collins[2], and Tal Arbel[1]

[1] Centre for Intelligent Machines, McGill University, Canada
[2] Montreal Neurological Institute, McGill University, Canada
[3] NeuroRx Research, Montreal, Canada

Abstract. The appearance of new Multiple Sclerosis (MS) lesions on MRI is usually followed by subsequent partial *resolution*, where portions of the newly formed lesion return to isointensity. This resolution is thought to be due mostly to reabsorption of edema, but may also reflect other reparatory processes such as remyelination. Automatic identification of resolving portions of new lesions can provide a marker of repair, allow for automated analysis of MS lesion dynamics, and, when coupled with a method for detection of new MS lesions, provide a tool for precisely measuring lesion change in serial MRI. We present a method for automatic detection of resolving MS lesion voxels in serial MRI using a Bayesian framework that incorporates models for MRI intensities, MRI intensity differences across scans, lesion size, relative position of voxels within a lesion, and time since lesion onset. We couple our method with an existing method for automatic detection of new MS lesions to provide an automated framework for measuring lesion change across serial scans of the same subject. We validate our framework by comparing to lesion volume change measurements derived from expert semi-manual lesion segmentations on clinical trial data consisting of 292 scans from 73 (54 treated, 19 untreated) subjects. Our automated framework shows a) a large improvement in segmentation consistency over time and b) an increased effect size as calculated from measured change in lesion volume for treated and untreated subjects.

1 Introduction

The appearance of new Multiple Sclerosis (MS) lesions visible on T2-weighted MRI is generally followed by a period of repair or lesion *resolution*, during which portions of the new lesion will return towards isointensity on MRI [1]. This resolution is thought to be due mostly to reabsorption of edema, but may also reflect other reparatory processes such as remyelination [1]. The percentage of new lesion that resolves has been posited as a marker for tissue repair and for staging disease [1]. Meier et al. have previously modeled the dynamics of new lesion formation on T2-weighted MRI and have observed a transient phase of 3-4 months, with larger lesions exhibiting a proportional greater amount of lesion resolution, and concentric patterns of resolution where voxels near the lesion boundaries are much more likely to resolve than those in the lesion center [1,2].

M.J. Cardoso et al. (Eds.): BAMBI 2014, LNCS 8677, pp. 118–129, 2014.

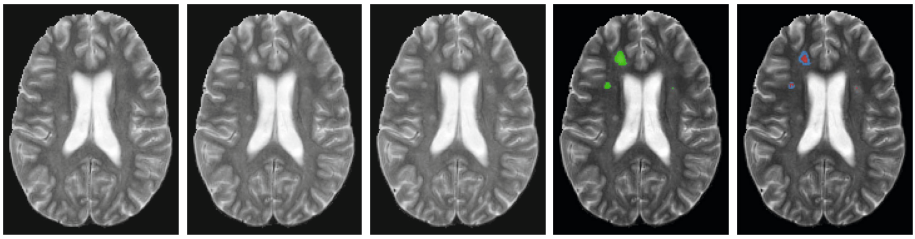

(a) screening **(b)** w24 **(c)** w36 **(d)** w24 **(e)** w36

Fig. 1. Example of new and resolving MS lesion on T2-weighted MRI over 3 timepoints. (a)-(c) show T2w images at screening, week 24 and week 36, while (d) and (e) overlay new and resolving lesion voxels at w24 and w36, where green denotes new, red denotes stable portions of new lesion and blue denotes resolving portions of new lesion, with respect to the previous timepoint.

An example of lesion formation and resolution over 3 serial scans is shown in Fig. 1.

Manual segmentation of MS lesion on MRI is time-consuming and subject to inter and intra-rater variability. Although many methods for automatic segmentation have been proposed [3], they remain imperfect, generally require substantive manual correction in real-world clinical environments, and still have relatively high degree of variability. Additionally, most methods do not take advantage of temporal relationships when considering multiple timepoints of the same subject, leading to reduced sensitivity to change and higher temporal segmentation variability, thus confounding inconsistent segmentation with real biological change. Several approaches have been proposed for the automatic segmentation of *new* MS lesions in sequential MRI [4], but little has been proposed for automatic detection of lesion resolution. While lesion resolution is implicitly modeled in [5], spatial and temporal characteristics of the resolution process are not modeled and the validation focuses exclusively on the detection of new lesions.

In this paper, we present a novel method for automatic detection of resolving lesion. A generative Bayesian model is used to detect resolving portions of lesions, where we consider MRI intensities, MRI intensity differences across time (difference images) and where we embed previously observed characteristics of lesions formation such as lesion size, time from lesion onset, and relative positions of voxels within a lesion [1].

Meaningful validation of any lesion segmentation algorithms is difficult due to the absence of a real ground truth. While manual references are often used for comparisons [3], these are generally imperfect, highly variable, and time-consuming to generate. The variability of lesion segmentations over timepoints of the same subject also makes them impractical as a basis for generating a reference for resolving lesion as most of the apparent resolution from one timepoint to the next would be attributable to inconsistent lesion boundaries rather than to veritable biological change. In the absence of an explicit reference segmentation for resolving

lesion voxels, we have chosen to combine our method with a method for new lesion detection [6] to provide a method for detection of lesion *change* in serial MRI. We compare lesion change measurements generated from our method to those derived from semi-manual reference segmentations lesions generated independently at each timepoint. We validate our method by comparing a) segmentation consistency across time and b) apparent treatment benefit as determined by effect size calculated from lesion volume change measurements from treated (N=54) and untreated (N=19) subjects in our test data.

2 Method

2.1 Bayesian Formulation

We present a Bayesian framework for automatic detection of resolving portions of lesions in serial MRI. We use a generative model where, at each voxel i in a lesion, we consider MRI intensities, $\boldsymbol{I_i^t}$, at the current timepoint and intensity differences, $\boldsymbol{D_i^t}$, between coregistered current and previous timepoints. We additionally consider the distance from lesion boundary, d_i, to model a concentric pattern of resolution, and lesion size at onset, s, to model the increased relative rates of resolution of larger new lesions. Finally we consider the time from lesion onset, a, to model the fact that most resolution occurs soon after lesion onset [7]. We define lesion onset as the time of first observation of a new lesion.

Resolution of Recently New Lesion

We first consider the case where we are provided with a set of new MS lesions that appear after our first available timepoint for a given subject, such that we can determine time of onset. In practice, these recently new lesions will be generated by an automated method as in [6]. We consider each lesion in the set of recently new lesions in turn, inferring the probability of resolution at each voxel i of the lesion, at all timepoints following lesion onset. Lesion size and boundaries are determined at lesion onset.

We allow two states for resolution status, res_i^t: a) *resolved*, corresponding to lesion that returned to "healthy" tissue from lesion at time t ($res_i^t = 1$), and b) *stable*, lesion which remains lesion at time t ($res_i^t = 0$). The distance from lesion boundary, d_i, is normalized based on lesion size and takes on a value between 0 (closest to lesion edge) and 1 (furthest from lesion edge) to provide invariance to lesion size.

For each voxel i in a given lesion, we wish to determine the probability of resolution at time t, based on observed MRI intensities at time t, $\boldsymbol{I_i^t}$, MRI intensity differences between times t and $t-1$, $\boldsymbol{D_i^t}$, as well as time since lesion onset, a, lesion size at onset, s, and distance from the lesion boundary, d_i:

$$
\begin{aligned}
&p(res_i^t|\boldsymbol{I_i^t}, \boldsymbol{D_i^t}, s, d_i, a) = \\
&= \frac{p(\boldsymbol{I_i^t}|res_i^t, \boldsymbol{D_i^t}, s, d_i, a)p(\boldsymbol{D_i^t}|res_i^t, s, d_i, a)p(s|res_i^t, d_i, a)p(d_i|res_i^t, a)p(res_i^t|a)}{p(\boldsymbol{I_i^t}|\boldsymbol{D_i^t}, s, d_i, a)p(\boldsymbol{D_i^t}|s, d_i, a)p(s|d_i, a)p(d_i|a)} \\
&= \frac{1}{K}p(\boldsymbol{I_i^t}|res_i^t)p(\boldsymbol{D_i^t}|res_i^t)p(s|res_i^t)p(d_i|res_i^t)p(res_i^t|a). \qquad (1)
\end{aligned}
$$

We have invoked Bayes' law multiple times, have treated the denominator as a normalization constant, and have made several statistical conditional independence assumptions:

- MRI intensity at time t is conditionally independent of $\boldsymbol{D_i^t}$,a,s, and d_i, given resolution status ($p(\boldsymbol{I_i^t}|res_i^t, \boldsymbol{D_i^t}, s, d_i, a)) = p(\boldsymbol{I_i^t}|res_i^t)$).
- MRI intensity difference $\boldsymbol{D_i^t}$ is conditionally independent of a,s, and d_i, given resolution status ($p(\boldsymbol{D_i^t}|res_i^t, s, d_i, a)) = p(\boldsymbol{D_i^t}|res_i^t)$).
- The lesion size is independent of normalized distance from lesion boundary and time from onset, given resolution status ($p(s|res_i^t, d_i, a) = p(s|res_i^t)$).
- The normalized distance from lesion boundary is conditionally independent of time from onset, given resolution status ($p(d_i|res_i^t, a) = p(d_i|res_i^t)$).

Our posterior probability of resolution at voxel i at time t is thus a product of 5 terms, each of which models the likelihood of resolution status based on one of intensity, intensity difference, distance from lesion boundary, lesion size, and time since lesion onset.

Lesion Resolution with Limited Scan History

In some instances, we may have no or insufficient scan history to determine which set of existing lesions are new and which are not (e.g. at first timepoint). In such cases, we assume that we are given a segmentation of all lesions at the first timepoint and we attempt to jointly infer which lesions are *recently new* at the first timepoint and resolution status at subsequent timepoints. We use RN_i^t to denote whether voxel i at time t corresponds to lesion that is recently new (< 6 months old) or not. Lesion newness, RN_i^t, is inferred by considering MRI intensities at the current timepoint and intensity differences between the current and ensuing timepoint, based on the observations that transient new lesions exhibit greater hyperintensity than stable older lesions and that this hyperintensity will decrease over time.

We can express the probability of being a recently new lesion at time $t-1$ based on MRI intensities at t and intensity difference between time t and time $t-1$ as:

$$
p(RN_i^{t-1}|\boldsymbol{I_i^{t-1}}, \boldsymbol{D_i^t}) = \frac{1}{K}p(\boldsymbol{I_i^{t-1}}|RN_i^{t-1})p(\boldsymbol{D_i^t}|RN_i^{t-1})p(RN_i^{t-1}), \qquad (2)
$$

where we have made conditional independence assumptions equivalent to those made for Eq. 1.

The boundaries of new lesions for which onset can be observed (i.e. at second or later timepoints) can be reliably determined even if they are confluent with existing lesion. However, for lesions where onset is not observed (i.e. lesions present at baseline), we cannot always reliably determine boundaries of individual lesions based on connectedness, especially for subjects with relatively high lesion load. As such, we choose not to consider lesion size and relative position of voxels in a lesion when determining probability of resolution in cases with insufficient scan history, as was done in Eq. 1. Incorporating our inference of lesion *newness*, we then infer resolution status for cases with insufficient scan history as:

$$\begin{aligned} p(res_i^t, RN_i^{t-1} | \boldsymbol{I_i^t}, \boldsymbol{D_i^t}, \boldsymbol{I_i^{t-1}}, a) &= p(res_i^t | RN_i^{t-1}, \boldsymbol{I_i^t}, \boldsymbol{D_i^t}, a) p(RN_i^{t-1} | \boldsymbol{I_i^{t-1}}, \boldsymbol{D_i^t}) \\ &= p(res_i^t | \boldsymbol{I_i^t}, \boldsymbol{D_i^t}, a) p(RN_i^{t-1} | \boldsymbol{I_i^{t-1}}, \boldsymbol{D_i^t}), \end{aligned} \tag{3}$$

where the right side of Eq. 3 is our inference of newness at time $t-1$ as determined by Eq. 2, and the left side is our inference on resolution determined as in Eq. 1 but without using size and distance from lesion boundary. Here we assume a time since lesion onset equal to the difference between time t and time $t-1$ and also assume that only lesion voxels inferred as new at time $t-1$ are candidates for subsequent resolution.

3 Experiments

3.1 Data Sets

We use a proprietary clinical trial data set in our experiments, consisting of 639 scans from 73 subjects with relapsing-remitting MS, where each subject considered minimally had scans at screening (s), week 24 (w24), week 36 (w36), and week 48 (w48). Most subjects had additional intermediate scans at some or all of w04, w12, w16 and w20. T1-weighted with (T1c) and without (T1w) gadolinium injection, T2-weighted (T2w), proton-density weighted (PDw), and T2w Fluid-Attenuated Inversion Recovery (T2w-FLAIR) scans were available at each timepoint. All scans were acquired axially with an in-plane resolution of 1mm and slice thickness of 3mm, underwent non-uniformity correction [8], brain masking [9] and were rigidly registered across MRI modalities and timepoints [10]. Additionally, all scans underwent a decile-based piecewise linear intensity normalization to a global intensity space [11]. Semi-manual lesion segmentations of all MS lesions were performed at some timepoints by trained experts prior to and independently of this study, where an initial segmentation of MS lesion was generated using [12] and then manually corrected following a strict protocol. Semi-manual segmentations were available for all 73 patients but only for timepoints screening, w24, w36, and w48. As such only these 4 timepoints were used for validation (292 scans total). Any additional intermediate timepoints

were included in the unsupervised training process. Treatment codes were made available for our data set, which identify subjects as either receiving treatment (N=54), or placebo (N=19). The availability of treatment codes allowed for validation based on effect size calculations, where we measure the statistical power of different measurements to differentiate treated and untreated (placebo) subjects.

Model Generation

Because we do not have ground truth for resolving lesion in our data set, we use an unsupervised approach to model learning. We first make use of existing software [6] to automatically identify new lesions in the entirety of our data set. This set of MS lesions, $\mathcal{L}_{new}$, then become candidates for resolution at timepoints following their appearance. We will consider model learning for inferring lesion resolution and inferring lesion *newness* separately, as different procedures are used for each.

Lesion Resolution Models

We use a hybrid unsupervised learning method where we first identify a set of representative samples of stable and resolving lesion voxels in our data, which we use to generate distributions for our intensity models, $p(\boldsymbol{I_i^t}|res_i^t)$, and intensity difference models, $p(\boldsymbol{D_i^t}|res_i^t)$. We then use these intensity based models to initialize our inference of resolution status at all voxels in $\mathcal{L}_{new}$ at timepoints following lesion onset, and use a generalized EM framework to learn parameters of our models for lesion size, normalized distance from lesion boundary, and lesion resolution conditioned on time since lesion onset.

Representative samples for stable and resolving lesions used for model initialization are generated using an approach based on difference of new lesions over 3 consecutive timepoints, as illustrated in Fig. 2. While such an approach is useful

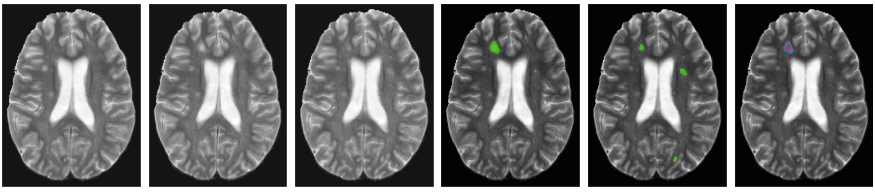

(a) $t1$ **(b)** $t2$ **(c)** $t3$ **(d)** new $t2$ **(e)** new $t3$ **(f)** stable / res

Fig. 2. Generating resolving and stable lesion samples using difference of new lesions. (a)-(c) show T2-weighted MRI of the same subject for 3 consecutive timepoints. (d)-(e) show new lesion (green) at $t2$ and $t3$ respectively, both with reference to $t1$. (f) shows resolving (blue) and stable (red) lesions samples at $t3$, where stable are those voxels that are identified as new in both (d) and (e), and resolving are those identified in (d) but not in (e).

for generating a set of samples, it is not a practical approach to detection of lesion resolution in the general case when considering additional (>3) timepoints, as it does not enforce temporal segmentation consistency and is not well suited to considering resolution occuring over multiple sequential timepoints.

Intensity based models are represented by 5 dimensional (corresponding to 5 modalities), 6-component Gaussian Mixture Models (GMMs), where the number of GMM components was chosen heuristically. Figure 3 shows learned probability densities for intensity and instensity differences, for resolving and stable (non-resolving) lesion voxels, marginalized over T2-weighted intensities.

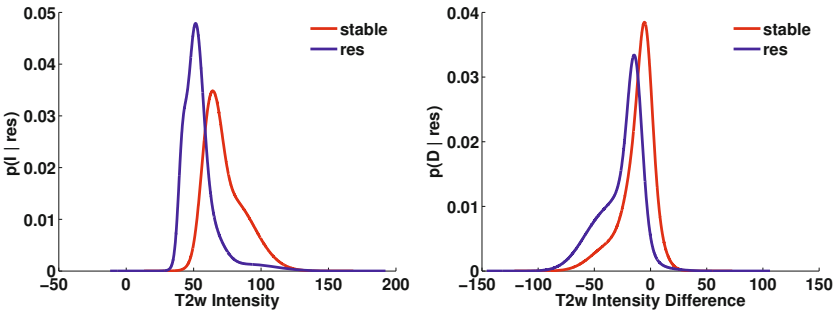

Fig. 3. (a) Intensity and (b) Intensity Difference densities for resolving and stable lesion voxels, shown marginalized over t2w for visulation purposes. In practice, models 5-dimensional densities corresponding to the 5 modalities used (T1w, T1c, T2w, PDw and T2w-FLAIR).

We use our intensity and intensity difference models to initialize resolution status of all voxels in $\mathcal{L}_{new}$ at timepoints following lesion onset. These initial estimates of resolution status will then act as hidden parameters in our EM learning framework. Model parameters for all our other models are then iteratively updated using generalized EM. The model learning process can be summarized as follows:

1. Generate a set of samples for resolving and stable lesion voxels using difference of new lesion.
2. Use samples generated in step 1 to generate models for intensity and intensity difference, for stable and resolved lesion voxels.
3. Generate a set of new MS lesions over all timepoints as candidates for resolution.
4. Initialize resolution status of new lesions generated in step 3 at all timepoints following onset, using only intensity and intensity difference models.
5. Initialize lesion size, normalized distance from lesion boundary, and resolution given time from onset models based on resolution status generated in step 4.

6. Use EM to iteratively update models, using models generated in step 5 as initializations. The E-step recalculates the probabilistic resolution status of new lesions based on the latest models and the M-step determines maximum likelihood models based on the updated resolution status.

We use a histogram based representation for our lesion size model, with 7 size ranges considered. We use exponential distributions to model both our normalized distance from boundary model and our resolution prior conditioned on lesion age.

Our EM framework jointly infers resolution status and model parameters. In our experiments, we have considered samples from the entirety of our data set (639 scans) for unsupervised model learning, but have only validated inference of resolution status in the subset of our data for which semi-manual lesion segmentations were available for comparison. Applying our learned models to a subset of the data from which they were learned can be considered as an additional E-step in our unsupervised learning framework.

Models for determining recently new lesion without scan history

We generate models for inferring lesion *newness* by generating intensity and intensity difference distributions for new and old (not recently new) lesions. We identify *old* lesions by considering voxels from a reference baseline lesion mask that remain lesion at least 6 months after baseline, or voxels from $\mathcal{L}_{new}$ that have not resolved 6 months after lesion onset. To identify *new* lesions we consider samples from $\mathcal{L}_{new}$ only at lesion onset and the subsequent timepoint. We again use 6 component GMMs to model our densities over the 5 modalities under consideration. Intensity and intensity difference models for new and old lesions are shown in Figure 4.

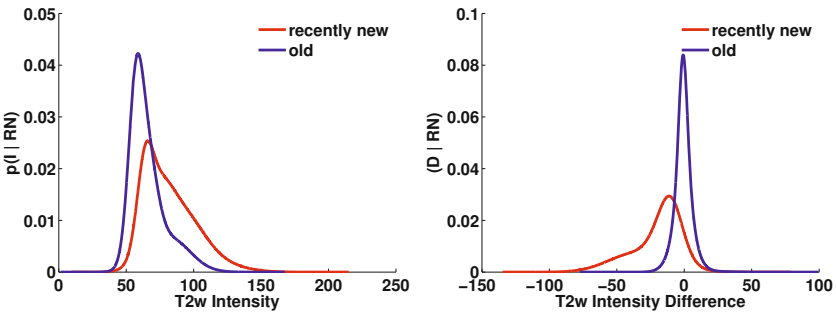

Fig. 4. (a) intensity and (b) intensity difference densities for new and old lesions, marginalized over t2w for visualization purposes. In practice, models 5-dimensional densities corresponding to the 5 modalities used (T1w, T1c, T2w, PDw and T2w-FLAIR).

3.2 Validation

Evaluating lesion resolution accuracy directly is not feasible due to the temporal variability in the available semi-manual reference lesion segmentations: most voxels identified as non-lesion at a given timepoint but as lesion in the previous timepoint would not actually correspond to resolving lesion but rather be due to temporal segmentation variability. As such, our validation focuses on measurements of lesion volume change over time, where we have coupled our method for detection of lesion resolution with an existing method for new lesion detection [6] to create a pipeline for lesion change detection in serial MRI based on change detection. We use the semi-manual reference segmentation as an initial lesion mask at our first timepoint, and lesion segmentation at subsequent timepoints is driven by detection of new, resolving and non-resolving (i.e. stable) lesion. Both lesion present at baseline and subsequently detected new lesions become candidates for resolution as determined by the proposed method. We compare the longitudinal segmentation of lesions as generated by our proposed pipeline based on change detection to the pre-existing semi-manual reference lesion segmentations. We validate based on a) segmentation consistency over time, and b) statistical power to differentiate treated from untreated subjects based on lesion volume change measurements.

Lesion Segmentation Consistency

Segmentation consistency is important as increased temporal variability will lead to less precise measurements of change over sequential scans. Segmenting lesions independently at each timepoint will lead to inconsistencies in lesion boundaries and in lesion detection, while modeling temporal dependencies via a change detection paradigm will provide a more consistent segmentation over time. We define new lesion volume between co-registered timepoints $t1$ and $t2$ as the volume of voxels that were not labelled as lesion at time $t1$ but were labelled as lesion at time $t2$. Similarily, we define resolving lesion volume as the volume of voxels that were labelled as lesion at time $t1$ but not at time $t2$. Table 1 shows new and resolving lesion volumes at w24, w36 and w48 using our method and using semi-manual lesion segmentations.

The proposed pipeline provides a much more temporally consistent segmentation of MS lesions, with the mean number of new and resolving lesion voxels detected over sequential timepoints both reduced by more than 90% as compared to semi-manual segmentations. Fig. 5 shows an example of a temporally consistent segmentation as generated by our method.

Effect Size Based on Measurements of Lesion Volume Change

Improved consistency of MS lesion segmentation is only useful if we can still detect veritable change. We demonstrate our sensitivity to change in lesion volume by calculating the effect size based on measurements of lesion volume change from screening to w48, as determined by our method and as determined from

Table 1. Lesion segmentation consistency as determined by mean volume of a) new lesion voxels (NV), and b) resolving lesion voxels (RV). Values represent mean volume in $mm^3 \pm 1$ standard deviation, evaluated over all 73 subjects. Values are shown for change over subsequent timepoints (s-w24, w24-w36, w36-w48). SM = semi-manual lesion segmentations, CD = Proposed method based on change detection.

	s-w24		w24-w36		w36-w48	
	NV	RV	NV	RV	NV	RV
CD	301±1036	243±892	102±505	68±293	55±208	55±288
SM	2364±2223	2427±2534	2158±2104	2171±2053	2159±2017	2203±2092

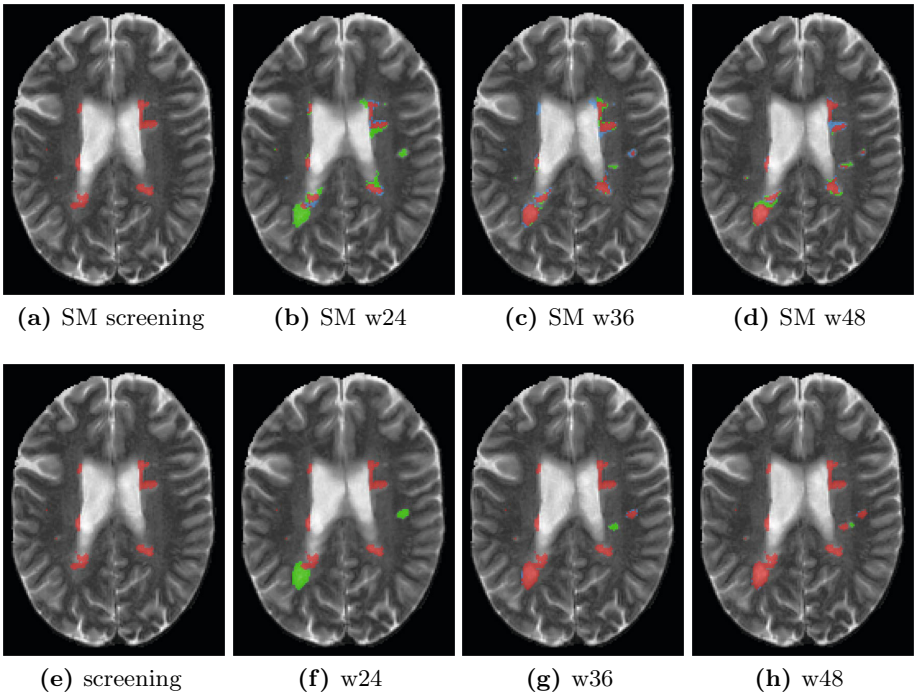

(a) SM screening **(b)** SM w24 **(c)** SM w36 **(d)** SM w48

(e) screening **(f)** w24 **(g)** w36 **(h)** w48

Fig. 5. Example lesion segmentations over 4 timepoints. (a)-(d) shows the semi-manual (SM) reference and (e)-(h) shows our proposed pipeline based on change detection. The SM segmentation is used as a baseline segmentation for both methods. Stable portions of lesion are shown in red, new lesion voxels are shown in green and resolving in blue, all with respect to the previous timepoint. The proposed method shows increased segmentation consistency across time while remaining sensitive to real change.

the semi-manual lesion segmentations. For our method, volume change is determined for each subject by taking the difference between cumulative new lesion volume and cumulative resolving lesion volume over the four timepoints.

For reference semi-manual segmentations, volume change is determined by taking the volume derived from the reference segmentation at w48 and subtracting from the volume derived from the reference segmentation at screening.

The effect size is estimated by Cohen's d with a pooled standard deviation [13], and represents a normalized measure of difference between the treated and untreated groups. While both methods show a positive treatment effect (i.e. treated subjects are shown to have a smaller change in lesion volume than untreated), the calculated effect size is larger (ES=0.77) when based on lesion volume change measurements generated by our proposed method, as compared to semi-manual segmentations (ES=0.44). This suggests that our method remains sensitive to lesion change and provides greater statistical power to differentiate treated and untreated subjects, as shown graphically in Fig. 6.

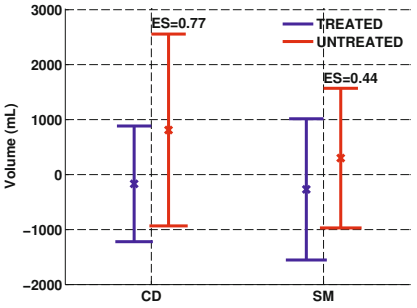

Fig. 6. Mean and standard deviation of lesion volume change from screening to w48 for treated (N=54) and untreated (N=19) subjects as measured from semi-manual lesion segmentations (SM) and the proposed method based on change detection (CD), along with corresponding effect size (ES) using Cohen's d.

4 Discussion

We have presented a novel method for detection of resolving MS lesion voxels in sequential brain MRI. By coupling our method with an existing method for detection of new MS lesions, we can provide a fully automated pipeline for determination of MS lesion volume change over serial scans based on change detection. Results demonstrate greater lesion segmentation consistency and improved statistical power to discriminate treatment arms using real clinical trial data, as compared to existing semi-manual segmentations. In addition, the ability to automatically detect resolving portions of MS lesions provides a potential measure of tissue repair, and as an aid for the analysis of MS lesion dynamics.

References

1. Meier, D.S., Weiner, H.L., Guttmann, C.R.: Time-series modeling of multiple sclerosis disease activity: a promising window on disease progression and repair potential? Neurotherapeutics 4(3), 485–498 (2007)

2. Meier, D.S., Guttmann, C.R.: MRI time series modeling of ms lesion development. Neuroimage 32(2), 531–537 (2006)
3. García-Lorenzo, D., Francis, S., Narayanan, S., Arnold, D., Louis Collins, D., Louis Collins, D.: Review of automatic segmentation methods of multiple sclerosis white matter lesions on conventional magnetic resonance imaging. In: Medical Image Analysis (2012)
4. Lladó, X., Ganiler, O., Oliver, A., Martí, R., Freixenet, J., Valls, L., Vilanova, J.C., Ramió-Torrentà, L., Rovira, À.: Automated detection of multiple sclerosis lesions in serial brain MRI. Neuroradiology 54(8), 787–807 (2012)
5. Elliott, C., Francis, S.J., Arnold, D.L., Collins, D.L., Arbel, T.: Bayesian classification of multiple sclerosis lesions in longitudinal MRI using subtraction images. In: Jiang, T., Navab, N., Pluim, J.P.W., Viergever, M.A. (eds.) MICCAI 2010, Part II. LNCS, vol. 6362, pp. 290–297. Springer, Heidelberg (2010)
6. Elliott, C., et al.: Temporally consistent probabilistic detection of new multiple sclerosis lesions in brain MRI. IEEE TMI 32(8), 1490–1503 (2013)
7. Meier, D., Weiner, H., Guttmann, C.: MR imaging intensity modeling of damage and repair in multiple sclerosis: relationship of short-term lesion recovery to progression and disability. American Journal of Neuroradiology 28(10), 1956–1963 (2007)
8. Sled, J., Zijdenbos, A., Evans, A.: A nonparametric method for automatic correction of intensity nonuniformity in MRI data. IEEE Transactions on Medical Imaging 17(1), 87–97 (1998)
9. Smith, S.: Fast robust automated brain extraction. Human Brain Mapping 17(3), 143–155 (2002)
10. Collins, D.L., Neelin, P., Peters, T.M., Evans, A.C.: Automatic 3D intersubject registration of MR volumetric data in standardized talairach space. Journal of computer assisted tomography 18(2), 192–205 (1994)
11. Nyul, L., Udupa, J., Zhang, X.: New variants of a method of MRI scale standardization. IEEE Transactions on Medical Imaging 19(2), 143–150 (2000)
12. Francis, S.: Automatic lesion identification in MRI of multiple sclerosis patients. Master's thesis, McGill University (2004)
13. Cumming, G.: Understanding the new statistics: Effect sizes, confidence intervals, and meta-analysis. Routledge, New York (2012)